

Immobilization of a Metal Complex in Y-Zeolite Matrix: Synthesis, X-ray Single-Crystal, and Catalytic Activities of a Copper (Schiff-Base)–Y Zeolite Based Hybrid Catalyst

Pratap Kumar Saha, Surajit Banerjee,[1] Sandip Saha, Alok Kumar Mukherjee,[1] Subramanian Sivasanker,[2] and Subratanath Koner*

Department of Chemistry, Jadavpur University, Jadavpur, Calcutta 700 032, India

[1]Department of Physics, Jadavpur University, Jadavpur, Calcutta 700 032, India

[2]Catalysis Division, National Chemical Laboratory, Pune 411 008, India

Received July 22, 2003; E-mail: skoner55@hotmail.com

A new zeolite-immobilized copper(II) complex catalyst has been prepared by entrapping [CuL] [LH_2 = *N*,*N*′-(1,1-dimethylethylene)bis(salicylaldiimine)] on NaY zeolite matrix. The reaction of Cu–NaY and molten LH_2 affords a green mass of crude catalyst that upon a treatment with CH_3CN gives a gray-colored hybrid catalyst (CuL–NaY). The prepared catalyst has been characterized by IR and UV–vis spectroscopic and EPR spectrometric measurements, TG–DTA analysis, powder X-ray diffraction, and surface-area measurements. To ascertain the structure of the immobilized complex, a single-crystal X-ray diffraction analysis of [CuL] was performed. Spectroscopic measurements showed that the green crude of CuL–NaY contains a penta- or hexa-coordinated copper(II) moiety, while the CuL–NaY catalyst contains a distorted square-planar [CuL] complex moiety. A remarkable catalytic activity of the prepared hybrid catalyst has been observed in oxidation reactions of 1-naphthol and norbornene.

The development of new functional materials by immobilizing selective chemical compounds in zeolitic or molecular-sieve matrices, which are expected to have exotic properties, like chromotropism, photoredox, photocatalysis or catalysis, has received much attention.[1–5] The immobilization of certain types of organic compounds in zeolite matrices has demonstrated a brilliant color change.[6] Recently, organic dye molecules have been immobilized in zeolite or a molecular sieve to prepare sensors.[7] Studies on the photochemical and photophysical properties of ruthenium complexes encapsulated in zeolite matrices have been undertaken by several groups.[8] It has been found that the said properties of neat metal complexes changed dramatically upon immobilization in zeolite matrices. Sykora et al. showed that the zeolite immobilized $[Ru(bpy)_n(bpz)_{3-n}]^{2+}$ complex (where bpz is 2,2′-bipyrazine and bpy is 2,2′-bipyridine) type hybrid materials can be used to store solar energy by a photochemical reaction.[8b] Studies on a zeolite-immobilized metal-complex based heterogeneous catalysts has received immense attention by a number of researchers in last two decades. Several interesting systems of this kind have been discovered.[1,2,9–11] To this end, metal complexes of porphyrins, phthalocyanines, Schiff-bases, etc. have been encapsulated into a zeolitic matrix for the development of efficient biomimetic oxidation catalysts, which have acted as a functional mimic of metalloenzymes.[12–15] The oxidation reactions catalyzed by metal complexes are often impeded due to oxidative degradation of the complex and/or the formation of μ-oxo dimers.[9] Several strategies, viz. encapsulation of those complexes within zeolitic[1,16] or polymeric matrices[17] or intercalation in clays,[1,18] have been adopted to enhance the stability and reactivity of such catalysts. It is now well understood that the encapsulation of these complexes in zeolitic hosts can enhance the catalytic performance of the complexes compared to their homogeneous counterparts used in solution.[9,14] Heterogenization of homogeneous catalysts in a porous solid support, like zeolite, makes the hybrid materials industrially important as new catalysts: a) can be reused in a catalytic process with its minimum loss; b) can be easily separated from the reaction mixture; c) they will be more robust than their homogeneous counterparts.[2,16] In an earlier communication we showed that the complex Cu(salen) [salen = *N*,*N*′-(ethylene)bis(salicylaldiimine)] encapsulated in NaY zeolite exhibits a novel color isomerism from green to red upon a treatment of the prepared hybrid material, Cu(salen)–NaY, with a specific solvent.[14] Subsequently, more reports concerning this type of color change of zeolite-immobilized metal-complex hybrid materials have been appeared in the literature.[19] The color change of the chromophoric groups originates from the steric obligations of the moiety inside the zeolite pores, most often due to the interaction of an axial ligand with the central metal ion. Interestingly a marked difference in the catalytic properties of the red and green species of Cu(salen)–NaY was observed in the oxidation reactions.[14] It has been postulated that the vacant trans axial positions facilitate a nucleophilic attack of the oxidant during a catalytic reaction.[19] However, such reports published so far have rarely stressed on understanding the stereo-electronic properties of the complex present in the zeolite supercage after immobilization. Knowledge regarding the structure of the immobilized complex is important to delineate the mechanism of the catalytic reactions and to design new catalysts of this kind. Such studies are scanty

Published on the web April 2, 2004; DOI 10.1246/bcsj.77.709

in the literature. Here we report the synthesis of [CuL] [LH_2 = *N*,*N*′-(1,1-dimethylethylene)bis(salicylaldiimine)], its X-ray crystal structure, immobilization of the [CuL] complex in the NaY zeolite matrix, and characterization of the prepared hybrid catalyst and its catalytic efficacy in oxidation reactions.

Experimental

Materials. NaY zeolite was procured from Tosoh Corporation, Japan. The ligand, *N*,*N*′-(1,1-dimethylethylene)bis(salicylaldiimine) (LH_2), was prepared from 1,1-dimethylethylenediamine and salicylaldehyde, following the standard condensation reaction procedure.[20] All other chemicals were of AR quality.

Synthesis of Complex [CuL]. A solution of (0.503 g, 2 mmol) $Cu(NO_3)_2 \cdot 3H_2O$ in methanol (20 mL) was slowly added to a methanolic (20 mL) solution of the Schiff base, LH_2 (0.613 g, 2 mmol), with constant stirring. The stirring was continued for another half an hour while violet-brown crystals were precipitated out. The crystals were collected by filtration, and were recrystallized from dichloromethane. Single crystals for X-ray analysis were grown from dichloromethane by slow evaporation technique. (Found: C, 60.82; H, 4.78; N, 7.80%. $C_{18}H_{18}N_2O_2Cu$ requires C, 60.41; H, 5.07; N, 7.83%); ν_{max}/cm^{-1} (KBr) 1630, 1605, 1535, 1460, 1449, 1380, and 1312. λ_{max}/nm (Nujol) 535 and 370.

Incorporation of Copper(II) in NaY. An aqueous solution of $Cu(NO_3)_2 \cdot 3H_2O$ (4.002 g) was stirred continuously for 5 h with NaY (4.107 g) in suspension. The white NaY zeolite turned to a bluish mass. The solid mass was then filtered and washed thoroughly with a large amount of deionized water using Soxhlet, and dried under vacuum to give a light-blue powder of Cu–NaY. The zeolite, thus produced, was then used for immobilization work.

Immobilization of [CuL] in NaY. The immobilization was done by the flexible ligand method (Scheme 1).[1] Cu–NaY (1.031 g) and 3.991 g of the required Schiff base (LH_2) were taken into a mortar and repeatedly ground and mixed intimately with each other. The whole mass then turned to a green powder. This was taken into a petridish and kept at 85 °C for half an hour. During heating the ligand, a Schiff base, was melted. The mixture was then cooled down when it was solidified. The melting process was repeated for 3–4 times mixing with some more ligand (LH_2) (ca. 0.5 g) each time. Finally, a green solid was obtained. This was thoroughly washed with acetonitrile using a Soxhlet. The solid residue was then dried under vacuum to give a light-gray powder hybrid catalyst (CuL–NaY).

X-ray Crystallography. Crystal data: $C_{18}H_{18}N_2O_2Cu$, M = 357.88, orthorhombic, space group *Pbca*, $Z = 8$, $a = 15.991(4)$, $b = 11.497(3)$, $c = 17.512(4)$ Å, $V = 3219.4(14)$ Å^3 (by least-square refinement of diffractometer setting angles for 57 automatically centered reflections $\lambda = 0.71073$), $D_{calcd} = 1.477$ g cm^{-3}, $F(000) = 1480$, $\mu = 1.367$ mm^{-1}, dark brown crystals, dimensions = 0.72 × 0.64 × 0.34 mm, $T = 293$ K.

Structure Determination: Intensities for 3424 reflections ($2.55° < \theta < 24.98°$) were collected using a Siemens P4 diffractometer ω scan mode with graphite-monochromated Mo Kα radiation. Data were corrected for Lorentz polarization and empirical absorption based on the ψ scan (T_{min}/T_{max}: 0.447/0.628) applied. Out of 2720 unique reflections ($R_{int} = 0.0636$) 2161 reflections with $I > 2\sigma(I)$ were considered. The structure was solved by the heavy atom method, and refined by full-matrix least-squares using SHELX-97.[21] The final refinement with all non-hydrogen atoms anisotropic and hydrogen atoms (placed at geometrical positions) held fixed with isotropic temperature factors converged to $R_1 = 0.0591$, $\omega R_2 = 0.1512$ for 2161 observed reflections ($R_1 = 0.0768$, $\omega R_2 = 0.1647$ for all reflections). The weighing scheme, $\omega = 1/[\sigma^2(F_0^2) + 0.1088P^2 + 0.9744P]$, where $P = (F_0^2 + 2F_c^2)/3$, gave satisfactory agreement.

Physical Measurements. Infrared and electronic spectra were measured on a Perkin Elmer 783 and Hitachi U 3400 spectrophotometer, respectively. EPR spectra were measured on a Varian E-112 EPR spectrometer at room temperature. Carbon, hydrogen, and nitrogen analyses were carried out with a Perkin Elmer 240C elemental analyzer. A TG–DTA study was performed on Shimadzu TG-50 thermogravimetric analyzer, a DTA-50 differential thermal analyzer and a Mettler Toledo Thermal Analyzer system. The X-ray powder-diffraction measurements were made on a PW 1730/1710 Philips XRD diffractometer. The copper content of the sample was estimated on a Varian Techtron AA-ABQ atomic absorption spectrometer. The catalytic reaction products were analyzed by an AIMIL 5700 NUCON and a Varian 3400 Gas Chromatograph equipped with an FID detector, and verified by a Shimadzu QP 5000 GCMS. Nitrogen adsorption measurements were made at 77 K using a Coulter Omnisorb 100 CX instrument.

Catalytic Reactions. The catalytic reactions were undertaken in a glass batch reactor. In a typical reaction, 1 g of the substrate was taken in 10 mL of CH_3CN, to which the catalyst (50 mg) was added. One mL of a 30% H_2O_2 solution was then added with continuous stirring. The products were collected at different time intervals, identified and quantified by GC, and verified by GC–MS.

Results and Discussion

Immobilization of the complex in a zeolite matrix was done by the "ship-in-the-bottle" technique.[1] A flexible Schiff base ligand (in the molten state) is allowed to react with copper(II) incorporated NaY zeolite (Scheme 1). It is expected that the [CuL] complex is formed in the supercage as well as on the surface of the Cu–NaY zeolite. Because the complex [CuL] is a neutral moiety, only a weak force, like electrostatic attraction, van der Waals interaction, etc. is operative here to catch hold of the complex on the surface of the zeolite. It seems that the Soxhlet extraction of the crude hybrid material with CH_3CN effectively washes away the complex molecule attached to the surface of the zeolite. However, the possibility of the presence of a small amount of copper(II) complex on the outer surface of the catalyst can not be ruled out, even after prolong washings. Nevertheless, complex molecules formed inside the zeolite su-

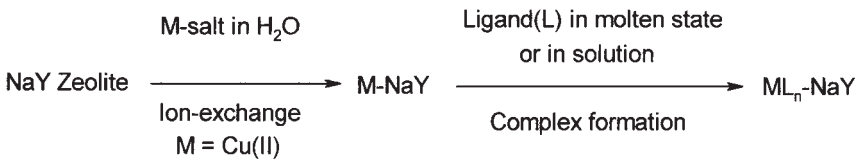

Scheme 1.

percage appear to remain in the matrix after prolong washings. A piece of evidence in support of this was obtained in surface-area measurements of the hybrid material. A significant decrease in the total surface area of the zeolite was observed upon immobilization of the complex (vide infra). Therefore, it can be postulated that most of the complex molecules in CuL–NaY are physically trapped inside the supercage of the zeolite. It is noteworthy that a sharp color change (light blue to green) of the Cu–NaY was observed during mixing with the melted ligand (vide supra). Upon washing (Soxhlet) with CH_3CN, the green-colored crude CuL–NaY catalyst turned to a gray powder. This type of color change of the hybrid materials upon a treatment with a certain solvent was also observed earlier.[14,19]

The elemental analysis of CuL–NaY showed the copper content of the catalyst to be 0.211% (by weight), whereas result of estimating the carbon and nitrogen in the prepared material supports the formation [CuL] in the zeolite matrix. This shows that about 50% of the supercages of NaY are occupied by the complex [CuL]. The copper complex present in the hybrid material acts as active centers of the catalyst.

X-ray powder diffraction measurements were performed for the NaY and CuL–NaY catalysts. A comparison of the XRD pattern of NaY and CuL–NaY shows that the crystallinity of the zeolite matrix almost remained intact after the formation of the complex in it. This indicates that the basic structure of the mother zeolite remain unaffected after immobilization; only the catalytically active copper complex moieties are sterically assembled in the zeolite matrix.

IR spectral measurements of [CuL] and CuL–NaY showed that all of the prominent bands for the azomethine group of the ligand appearing in the region 1600–1300 cm^{-1} of the [CuL] species are also present in CuL–NaY. These bands can be regarded as being a signature of the complex, because no zeolitic IR band appears in this region of the spectra, except for the band for HOH bending of H_2O at 1650 cm^{-1}. Upon careful drying of the prepared catalyst, this band (at ca. 1650 cm^{-1}) disappears. The vibration bands of the host zeolite obscured the IR bands of the complex in other regions.

The electronic spectra of the species [CuL], CuL–NaY catalyst, and green crude of CuL–NaY are given in Fig. 1. The peaks appearing at 535 nm and 370 nm in the electronic spectra of [CuL] are interpreted as being the d–d transition and ligand charge-transfer bands, respectively. In the case of CuL–NaY, the d–d band appeared at ca. 537 nm, whereas upon immobilization the charge-transfer band was shifted to a shorter wavelength region and appeared at 345 nm. This type of shifting of the charge-transfer band after immobilization of a certain complex in the zeolite matrix was observed earlier.[14] On the other hand, the electronic spectra of the green-colored crude CuL–NaY showed three peaks at 550, 400(sh), and 320 nm (Fig. 1). The shift of the d–d transition towards a longer wavelength region in the case of crude CuL–NaY indicates a lowering of the in-plane ligand field around the copper(II) ions. It is well documented that such a type of shifting usually occurs due to an increase of the axial ligand interaction with copper(II) ions.[22] It is noteworthy that in the case of copper(II) Schiff-base complexes it has been observed that the green species generally possess a penta-coordinated copper(II) moiety, whereas red species possess a tetra-coordinated one.[23] Therefore, it can be

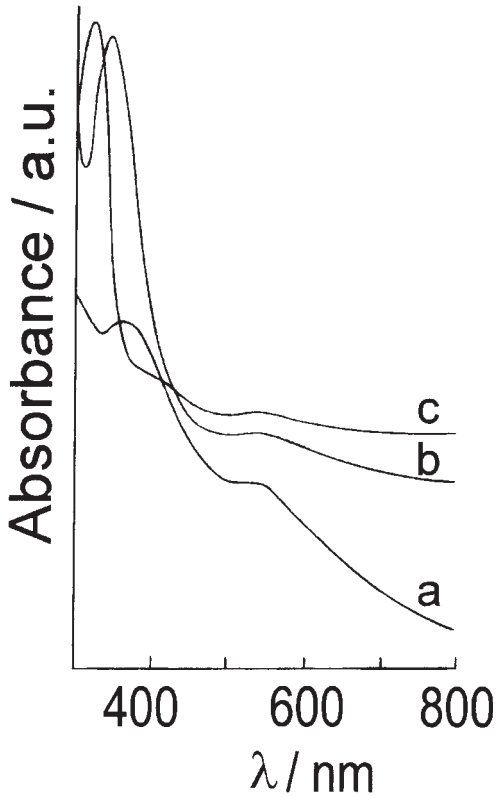

Fig. 1. UV–vis spectra of the pristine complex [CuL] (a); CuL–NaY (b); green crude product of CuL–NaY (c).

assumed that the crude product of CuL–NaY contains a six or five coordinated copper(II) moiety in addition to the square planar [CuL].

The EPR spectra of the species [CuL], CuL–NaY, and green crude of the catalyst are given in Fig. 2. The principal g values, calculated by usual methods from the EPR spectra, are in good agreement with those reported for copper(II) Schiff-base complexes.[24] The $g_{\parallel}$ and $g_{\perp}$ values of the pristine complex, CuL–NaY catalyst, and green crude of CuL–NaY are 2.252, 2.256, 2.124 and 2.197, 2.162, 2.096, respectively. The g values of the catalyst CuL–NaY is significantly higher than that of its green crude product. It is well understood that a decrease in the axial ligand interaction with the copper(II) center in these types of complexes leads to an increase in $g_{\parallel}$.[22a,c,24] Therefore, this difference is not inconsistent with the observations in electronic spectral measurements. The difference in the line width of the EPR spectra of [CuL] and CuL–NaY indicates that the copper complex in the zeolite matrix suffers a slight distortion upon immobilization. Such an increase in the line widths is usually observed as the result of a shortening of the relaxation time (T_1) of unpaired electron of copper(II) in case the complex moiety undergoes a tetrahedral distortion.[25]

The thermogravimetric (TG) measurement and differential thermal analysis (DTA) of the complex [CuL], CuL–NaY, and green crude product of CuL–NaY are shown in Fig. 3. The DTA curve of the [CuL] shows two prominent exothermic peaks at ca. 220 and 310 °C. The corresponding weight losses are observable in the TG curve of the thermogram of [CuL]. The TG curve of CuL–NaY shows a significant weight loss in the temperature range 30–200 °C; a gradual loss is then ob-

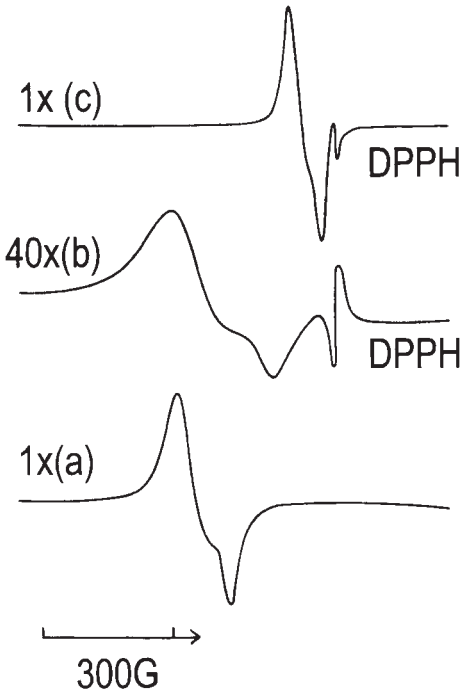

Fig. 2. EPR spectra of the complex [CuL] (a), CuL–NaY (b), and green crude product of CuL–NaY (c). The signal gain for CuL–NaY (b) was 40 times higher than that of the complex [CuL] or the green crude product.

served up to 600 °C. The corresponding DTA curve shows no observable peak up to 200 °C, but a prominent exothermic peak is observed at ca. 230 °C. On the other hand, the crude product of CuL–NaY showed a weight loss of ca. 57% in the temperature range 30–300 °C; the weight loss continued up to 600 °C and a total loss has been recorded for this sample, ca. 78%. This shows the green species contains a large amount of adsorbed H_2O in addition to the copper(II) Schiff-base complexes. Two endothermic and one exothermic peaks were observed in the DTA curve of the green species of CuL–NaY at ca. 92, 250, and 372 °C, respectively. The DTA profiles of the crude CuL–NaY and CuL–NaY catalyst are completely different from the corresponding DTA profile of the pristine complex [CuL]. Therefore, it can be concluded that the thermal behavior of the pristine complex changes considerably upon immobilization in zeolite matrix.

An ORTEP[26] diagram of the complex [CuL] along with the atom numbering scheme is given in Fig. 4. The selected bond distances and angles of the complex are listed in Table 1. The coordination geometry around the copper atom can be described as a distorted square-planar geometry. Two nitrogen atoms of the azomethine groups of the ligand and the two oxygen atoms of the phenoxo groups of the salicylaldehyde substructure of the ligand occupy the four coordination sites of the central metal ion. The copper atom is slightly displaced from the plane consisting of N1, N2, O1, and O2 atoms. The distortion is also apparent in the inequality of the bond lengths of two oxygen donor atoms and two nitrogen donor atoms. The copper(II) complexes of Schiff bases often form a dimer through a semicoordinated axial bond between the copper(II) ion of one complex moiety and the phenoxo group of its nearest

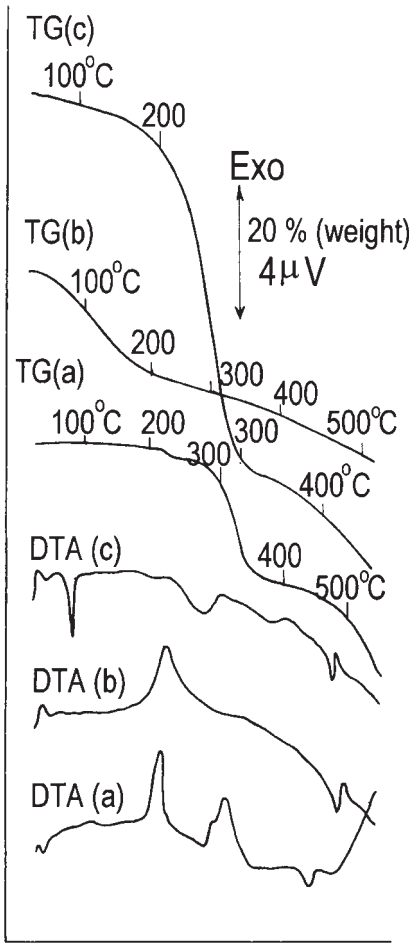

Fig. 3. TG–DTA curves of [CuL] (a), CuL–NaY (b), and green crude product of CuL–NaY (c). Sample taken = 10.00 mg. Rate of heating = 10 °C/min. α-Al_2O_3 was taken as the reference solid.

neighbor.[23] It is well established that the formation of such a dimer often deactivates the copper complexes in catalytic oxidation reactions.[9] Nevertheless, no such intermolecular interaction was observed between the copper(II) ion and the phenoxo group in the present complex.

Surface-area measurements give valuable information about the immobilization of the complex in a zeolite matrix.[27] A nitrogen sorption experiment showed a remarkable decrease in the surface area of the immobilized materials compared to the original NaY zeolite in the present case. Nitrogen is generally adsorbed in the micropores as well as the outer surface of the zeolite. Thus, if the complex [CuL] occupies the pores of the NaY zeolite in CuL–NaY, a smaller amount of gas will be adsorbed by the catalyst. Indeed this happens in the case of CuL–NaY. The total surface area of the original NaY was 770 $m^2\,g^{-1}$ upon immobilization of the complex into it this value decreases to ca. 451 $m^2\,g^{-1}$.

All the above-mentioned results convincingly demonstrate the presence of the copper(II) Schiff-base moiety in the prepared catalyst, CuL–NaY. Spectroscopic analyses indicate that the green-colored crude of CuL–NaY most probably contains the penta- or hexa-coordinated form of the copper(II) Schiff-base moiety. Although virtually no difference is observed in

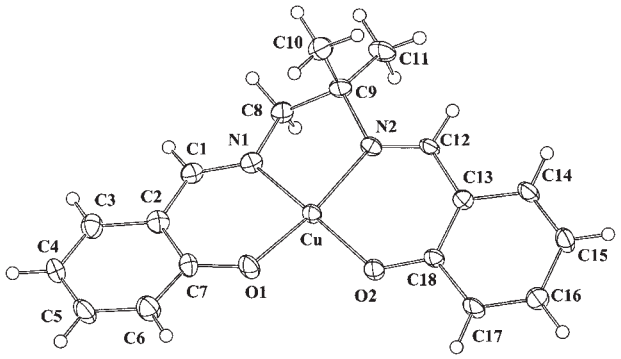

Fig. 4. ORTEP diagram of [CuL] showing atom numbering scheme.

Table 1. Selected Bond Lengths (Å) and Angles (°) for [CuL]

	Bond lengths/Å		
Cu–O(2)	1.894(3)	Cu–N(1)	1.940(3)
Cu–O(1)	1.899(3)	Cu–N(2)	1.942(4)
	Bond angles/°		
O(2)–Cu–O(1)	88.80(13)	N(1)–Cu–N(2)	85.0(2)
O(2)–Cu–N(1)	170.30(14)	O(1)–Cu–N(2)	166.06(14)
O(1)–Cu–N(1)	93.7(2)	O(2)–Cu–N(2)	94.83(14)

Table 2. Catalytic Performance of CuL–NaY[a)]

Catalyst	Reaction time/h	Conversion (mass/%)	Product distribution (mass/%)			
			Norbornene epoxide		1,4-Naphtho-	1,4-Dihydroxy-
			exo-	*endo*-	quinone	naphthalene
CuL–NaY	3	21.6	21.6	—		
	12	52.3	52.3	—		
	3	10.5			10.5	—
	12	19.8			19.8	—
[CuL]	12	28.0[b)]	13.8	12.1		
		12.5[b)]			6.9	4.8
CuL–NaY (Green)	12	No detectable activity[c,d)]				
Cu–NaY	12	No detectable activity[d)]				

a) No Cu-leaching during reaction. b) This includes some other minor oxidized products. c) Reactions were performed in CH_3OH medium. d) Cu–NaY and crude CuL–NaY (Green) species showed no catalytic activity towards epoxidation of norbornene and oxidation of 1-naphthol.

the d–d transition band of the [CuL] and CuL–NaY catalyst in their electronic spectra, upon immobilization the ligand charge-transfer band of the copper(II) Schiff-base moiety showed a red-shift of the band. The difference is more apparent between these two species in their EPR spectra, which is attributable to a tetrahedral distortion of the copper(II) Schiff-base moiety. An X-ray single-crystal analysis showed that the dimensions of the [CuL] complex are ca. 12×7 Å. It is well-known that the size of the supercage of NaY is ca. 12 Å; therefore, some amount of distortion of the immobilized complex is not unexpected. However, it may be emphasized that upon immobilization the [CuL] complex retains its tetra-coordination ligand environment around the copper(II) ions.

The epoxidation of norbornene and the hydroxylation of naphthol were carried out to test the catalytic efficiency of the prepared catalyst. The results of the reactions are given in Table 2. In both reactions, the hybrid catalyst showed good catalytic activity. It is interesting to note that neither the green-colored crude CuL–NaY (in methanol medium) nor the Cu-exchanged mother zeolite (Cu–NaY) exhibited any noticeable catalytic activity. However, the pristine [CuL] showed catalytic activity in solution in the above-mentioned oxidation reactions, though the catalytic efficiency was much lower than its hybrid analogue, CuL–NaY (Table 2). It should be noted that an atomic-absorption spectroscopic analysis shows that copper is not leached out during oxidation reactions because no copper was detected in the liquid phase of the reaction mixture after the completion of the reaction.

It is evident from this study that the copper(II) complex immobilized in the NaY matrix possesses a distorted square-planar coordination environment. The chromotropism showed by the green-colored CuL–NaY crude species upon a treatment with CH_3CN is due to the chromophoric change of copper(II) ions. Most probably, a transformation from penta- or hexa-coordination to a tetra-coordination environment around the copper(II) ions occurrs during the chromotropic change. In an earlier study we observed a similar kind of chromotropism in Cu(salen)–NaY. Based on the spectroscopic results it was postulated that the immobilized species, which is catalytically active, might possess a square-planar environment around the copper(II).[14] However, we could not isolate the tetracoordinated copper(II) complex in its pristine form in case of the Cu(salen) to justify, spectroscopically or structurally, whether the red species of Cu(salen)–NaY really contains the tetracoordinated copper(II) Schiff-base moiety. This study shows that the catalytically active species indeed possesses a square-planar copper(II) center. This strengthens our postulate that a square-planar copper(II) complex moiety with its two vacant axial positions facilitates a neucleophilic attack by the oxidant to enhance the catalytic activity of the hybrid materials in the oxidation reactions.

The work was financially supported by the CSIR, New Delhi, by a grant (01(1674)/00/EMR-II) to SK. PKS thanks CSIR for a research fellowship.

References

1 F. Bedioui, *Coord. Chem. Rev.*, **39**, 144 (1995).
2 J. M. Thomas, *Angew. Chem., Int. Ed.*, **38**, 3588 (1999).
3 M. Borja and P. K. Dutta, *Nature*, **42**, 362 (1993).
4 V. Ramamurthy, D. R. Sanderson, and D. F. Eaton, *J. Am. Chem. Soc.*, **115**, 10438 (1993).
5 a) M. Nakamura, T. Tatsumi, and H. Tominaga, *Bull. Chem. Soc. Jpn.*, **63**, 3334 (1998). b) E. A. Kozlov, A. Kozlov, K. Asakura, and Y. Iwasawa, *J. Mol. Catal. A: Chem.*, **137**, 223 (1999). c) A. Kozlov, K. Asakura, and Y. Iwasawa, *Chem. Lett.*, **1997**, 313. d) J. Guzman and B. C. Gates, *Dalton Trans.*, **2003**, 3303, and references therein.
6 V. Ramamurthy, P. Lakshminarasimhan, C. P. Grey, and L. J. Johnston, *Chem. Commun.*, **1998**, 2411, and references therein.
7 a) J. L. Meinershagen and T. Bein, *J. Am. Chem. Soc.*, **121**, 448 (1999). b) B. Meier, T. Werner, I. Klimant, and O. S. Wolfbeis, *Sens. Actuators, B*, **29**, 240 (1995).
8 a) J. A. Incavo and P. K. Dutta, *J. Phys. Chem.*, **94**, 3075 (1990). b) M. Sykora and J. R. Kincaid, *Nature*, **387**, 162 (1997). c) M. Sykora, K. Maruszewski, S. M. Treffert-Ziemelis, and J. R. Kincaid, *J. Am. Chem. Soc.*, **120**, 3490 (1998).
9 K. Balkus, Jr., M. Eisa, and R. Levedo, *J. Am. Chem. Soc.*, **117**, 10753 (1995).
10 a) K. Balkus, Jr., A. G. Gabrilov, S. L. Bell, F. Bedioui, L. Rové, and J. Devynck, *Inorg. Chem.*, **33**, 67 (1994). b) K. Ebitani, K. Nagashima, T. Mizugaki, and K. Kaneda, *Chem. Commun.*, **2000**, 869. c) D. E. De Vos, M. Dams, B. F. Sels, and P. A. Jacobs, *Chem. Rev.*, **102**, 3615 (2002), and references therein.
11 a) R. Raja and P. Ratnasamy, U. S. Patent 5767320 (1998). b) P. Ratnasamy and R. Raja, EP 0784045 (1998).
12 N. Herron, *CHEMTECH*, **1989**, 542.
13 B. M. Weckhuysen, A. Verberckmoes, I. P. Vannijvel, J. A. Pelgrims, P. L. Buskens, P. A. Jacobs, and R. A. Schoonheydt, *Angew. Chem., Int. Ed. Engl.*, **34**, 2652 (1995).
14 S. Koner, *Chem. Commun.*, **1998**, 593.
15 C. A. Tolman, J. D. Droliner, M. J. Nappa, and N. Herron, "Activation and Functionalisation of Alkanes," ed by C. L. Hill, Wiley, Chichester (1989), p. 303.
16 a) P. C. H. Mitchell, *Chem. Ind. (London)*, **1991**, 308. b) J.-M. Brégeault, *Dalton Trans.*, **2003**, 3289, and references therein.
17 R. F. Parton, I. F. Vankelecom, M. J. Casselman, C. P. Bezoukhanova, J. B. Uytterhoeven, and P. A. Jacobs, *Nature*, **370**, 541 (1994).
18 J. B. Yoon, S. H. Whang, and J. H. Choy, *Bull. Korean Chem. Soc.*, **21**, 989 (2000).
19 S. Deshpande, D. Srinivas, and P. Ratnasamy, *J. Catal.*, **188**, 261 (1999).
20 a) R. H. Holm, G. W. Everett, and A. Chakravorty, *Prog. Inorg. Chem.*, **7**, 83 (1965). b) R. H. Bailes and M. Caovin, *J. Am. Chem. Soc.*, **69**, 1886 (1947).
21 G. M. Sheldrick, "SHELXS-97: A Program for Crystal Structure Determination," University of Göttingen, Germany (1997).
22 a) R. L. Belford, M. Calvin, and G. Belford, *J. Chem. Phys.*, **26**, 1165 (1957). b) L. Febbrizzi, M. Micheloni, and P. Paoletti, *Inorg. Chem.*, **13**, 3019 (1974). c) D. R. Bloomqueist and R. D. Willett, *Coord. Chem. Rev.*, **47**, 125 (1982).
23 M. M. Bhadbhade and D. Srinivas, *Inorg. Chem.*, **32**, 6122 (1993).
24 a) A. H. Maki and B. R. McGarvey, *J. Chem. Phys.*, **29**, 35 (1958). b) E. Hasty, T. J. Colburn, and D. N. Hendrickson, *Inorg. Chem.*, **12**, 2414 (1973). c) H. Yokoi, M. Sai, and T. Isobe, *Bull. Chem. Soc. Jpn.*, **42**, 2232 (1969).
25 B. J. Hathaway and D. E. Billing, "Transition Metal Chemistry," ed by R. L. Carlin, Elsevier, Amsterdam (1970), Vol. 5, p. 199.
26 C. K. Johnson, "ORTEP, Report ORNL-5138," Oak Ridge National Laboratory, Oak Ridge, TN (1976).
27 R. Ferreira, M. Silva, C. Freire, B. de Castro, and J. L. Figueiredo, *Microporous Mesoporous Mater.*, **38**, 391 (2000).